M. KORNIENKO, A. NAUMENKO
Taras Shevchenko National University of Kyiv
(64, Volodymyrs'ka Str., Kyiv 01601, Ukraine)

THE VIBRATIONAL BAND ENHANCEMENTS FOR ACTIVE AND "SILENT" VIBRATIONS IN THE RAMAN AND IR SPECTRA OF FULLERENE C_{60} NANOFILMS

UDC 535.34, 535.37, 667.287.4

A comparison of the intensities of the vibrational bands (VB) in Raman and IR spectra for nanofilms of C_{60} 150–250 nm in thickness and for microfilms 1–2 μm in thickness has been done. In the Raman spectra of nanofilms, the enhancement of the active bands Hg(1 ÷ 8) by 2 ÷ 7 times in comparison with a slight weakening of the Ag(1,2) band for microfilms has been observed. It is shown that the Raman and IR vibrations Gg,u, Hu, $F_{1,2}g$, and F_2u, which are inactive for icosahedral symmetry I_h, and the lateral spectral components of the bands Hg(1 ÷ 8) increase by 5–50 times and more. The observed phenomena is associated with the significant changes in the electro-physical properties of nanostructured media due to a weakening of the symmetry and an increase in the anharmonicity and the nonlinear interaction of vibrational modes. During the polymerization of a nanofilm by diamine (N_2H_4), the observed enhancement of VB decreases due to a decrease in the vibrational nonlinearity. The differences between the experimental intensities of VB and the results of quantum-chemical calculations are discussed.

Keywords: nanofilm, fullerene, enhancement of vibrational bands, vibrational-electronic interaction, induction of electronic bands, nonlinear interaction of vibrational modes.

1. Introduction

The manifestations of a vibrational anharmonicity in large molecules such as biological macromolecules, a C_{60} fullerene molecule, and nanoparticles differ significantly from those in simple molecules. This is due to a large number of vibrational modes and an easy implementation of different vibrational resonances [1, 2]. The latter leads to a strengthening of the vibration-electron coupling [3], resulting in a completely new manifestation of the anharmonicity due to changes in the electronic states. Furthermore, these phenomena in the nanostructures are complicated due to the formation of phonon dispersion branches [4]. Naturally, together with the anharmonicity, the nonlinear susceptibility of nanostructured media in the vibrational field undergoes changes. At the nonlinear resonant interaction of thermally excited low-frequency vibrational modes, the higher vibrational states (overtones and sum tones) are generated, and these states approach the electronic states (ES) and effectively interact with them [3]. In this case, the change of ES consistent with vibrational excitations promotes an anomalous increase in the vibrational nonlinearity, which leads to the phenomenon of strong vibration-electron interaction (VEI) [1–3]. It should be noted that the efficiency of nonlinear wave processes significantly increases in the presence of many vibrational resonances, as well as significant spatial accumulation wave processes, which distinguishes them from local non-linearities. In particular, in fullerene C_{60}, a number of serial vibrational resonances of the Hg(1) + Hg(2) = Hg(3), Hg(1) + Ag(1) = Hg(4), 2Hg(3) = Hg(7), Hg(3) + + Hg(4) ≈ Ag(2), 2Hg(4) ≈ Hg(8), *etc.* [1, 2] has been realized, which improves the efficiency of a non-equilibrium excitation of vibrational states and the higher influence of VEI. However, the role of the nonlinear interaction between vibrational modes (NIVM) in nanostructures, particularly, in the typical carbon materials (fullerenes, nanotubes, graphene, *etc.*) still remains poorly understood. We point out that the general patterns of the spatial dynamics of nonlinear resonant wave interactions were previously studied in many works [5–8] in detail. This will allow us to establish the effect of the elevated vibrational anharmonicity of atoms in nanostructures and a possible

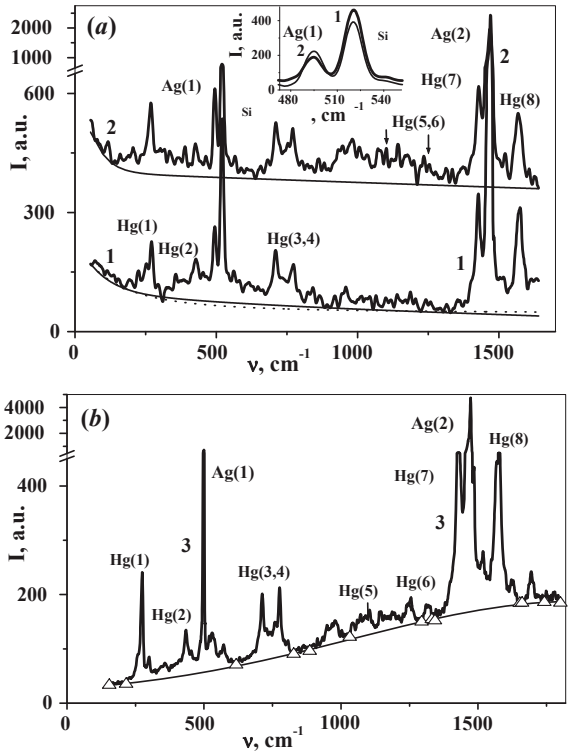

Fig. 1. Extraction of the wide electronic bands (EB) in the Raman spectra of C_{60} nanofilms with thicknesses of about 200 nm under hot (1) and cold (2) deposition processes (*a*) and microfilms with a thickness of 2 microns (*b*). The inset shows the Raman bands of breathing vibration Ag(1) and Si of crystalline silicon substrates for a C_{60} nanofilm

change of the electronic states as a result of the amplification of the nonlinear interaction of vibrational modes and the vibrational-electronic interaction.

2. Experimental Procedure and Numerical Processing of Spectral Data

C_{60} films were deposited on substrates of crystalline silicon by hot or cold deposition. The Raman spectra were studied using automated spectrometers DFS-24 with a cooled photomultiplier and a photon counting system. Raman spectra were excited by an Ar^+ laser with the wavelengths $\lambda_L = 514.5$ and 488 nm. To reduce the influence of the photopolymerization of C_{60}, the cylindrical focusing of the laser radiation (spot size of 0.3×2.5 mm^2) was used; laser intensity was 2 W/cm^2. At the sharp focusing of laser excitation $\lambda \sim 1$ mW up to a diameter of 2 microns, the exciting radiation intensity exceeds 10 kW/cm^2, which allows us to study the impact of light radiation on the Raman spectra and the VEI. IR spectra of C_{60} have been studied by a Fourier spectrometer Nicolet NEXUS-470. In Raman and IR spectra of the nanostructures, there is a broadband background, as a rule. It is seen in Fig. 1 *a, b*, which gives the overview of the Raman spectra of C_{60} nanofilms. Previously, we have established the electronic nature of the broadband background in RS [1–3]. For RS of C_{60} nanofilms, the intensity of the broadband background decreases with an increase of the frequency, as shown in Fig. 1, *a*. It is characteristic that, under the hot method of NF deposition, the background in a high frequency region is almost two orders lower by magnitude (see spectrum in Fig. 1, *a* than at the cold deposition method (upper spectrum 2). For the studied microfilm with a thickness about 2 microns, the wide electronic band is well approximated by a Gaussian $I_F = I_0 + A\exp[-(\nu - \nu_0)^2/2(\delta\nu)^2]$ with a maximum in the region of the most intense Raman Ag(2) and Hg(7,8). The half-width of the considered electronic band (EB) $\delta\nu = 1650$ cm^{-1} is comparable with the frequency $\nu_0 = 1870$ cm^{-1}, which characterizes the observed broadband EB, being much wider than the vibrational bands. Note that, after the polymerization of C_{60} nanofilms by hydrazine N_2H_4, the intensity of the broad EB increases with the frequency OS, as in the case of microfilms.

For C_{60} nanofilms, the line $\nu_{Si} = 520$ cm^{-1} of the crystalline silicon substrate is observed together with the line of radial breathing mode Ag(1) at 497 cm^{-1}. This is shown in the inset in Fig. 1, *a* in detail. The line ν_{Si} can be used to classify the C_{60} nanofilms by thickness (d). As d decreases, the intensity of ν_{Si} decreases as well. For a microfilm of C_{60} about 1.2–2 microns in thickness, this line disappears (Fig. 1, *b*). In order to increase the signal/noise ratio, the numerical analysis of the spectra was carried out with optimal numerical smoothing. In the numerical decomposition of vibrational and electronic bands on the individual spectral components, the method of least squares with variations of the frequency positions of the components, their intensities, shapes, and half-widths has been used.

3. Results and Discussion

3.1. Enhancement of active vibrational bands in the Raman spectra of C_{60} nanofilms

For the correct comparison of the intensities of various vibrational bands of C_{60} films, the normaliza-

tion of indicated lines $I_N = I/I_{\max}$ on the intensities of the strongest Raman and IR lines of Ag(2) (1469 cm^{-1}) and $F_1u(1)$ (527 cm^{-1}) has been conducted. The comparizion of some Raman and IR bands for nano- and microfilms of C_{60} are shown in Fig. 2, *a, b*. It is obvious that, in C_{60} nanofilms, the low-frequency bands Hg(1,2) and middle-frequency Hg(3,4) and high-frequency Hg(7,8) bands are much more intense than those in microfilms. It is worth noting a weakening of the Hg(3) band intensity, an increase of the Hg(4) band intensity under the polymerization of nanofilms 1 and 2 by diamine N_2H_4 (see Fig. 2, *b*), and the observation of a series of RS inactive vibrations, for example Gu(2), Gg(1,3). Moreover, the inactive vibrations have appreciable intensities, which became significantly weaker at the polymerization of nanofilms and are virtually absent in microfilms.

The main part of the obtained results on the vibrational band enhancement in Raman spectra of nanofilms of fullerene C_{60} is summarized in Fig. 3. There are the ratios of maxima of active Hg(1–8) vibrations in different nanofilms and a microfilm with $d = 2$ μm under study. According to the numbering of the spectra adopted in Figs. 1 and 2, the relation 1/3 in Fig. 3 belongs to a hot-deposited nanofilm, 2/3 belongs to cold-deposited films, and the relations 1p/3 and 2p/3 belong to polymerized nanofilms. It is evident that a significant enhancement of the vibrational bands is achieved for the vibrations Hg(1,2), Hg(3,4), and Hg(7,8). According to Fig. 3 the intensities of the Raman-active Hg(j), where $j = 1 \div 8$, in nanofilms of fullerene C_{60} are enhanced by 2–7 times as compared with the microfilm, with a small increase of the intensity of the whole symmetric vibration Ag(1) (see also Fig. 2, *b*). For the nanofilms polymerized by diamine N_2H_4, the enhancement of the bands stay weaker due to a weakening of the vibrational nonlinearity.

3.2. Abnormal enhancement of the bands of "silent" vibrations in IR and Raman spectra of the nanofilms of fullerene C_{60}

The abnormally strong increase of many vibrations Gg,u, Hu, $F_{1,2}g$, F_2u, *etc.* inactive for icosahedral symmetry I_h has been also observed in Raman and IR spectra, as illustrated in Fig. 4 *a, b*. All IR spectra have been normalized to the absorbance of the most

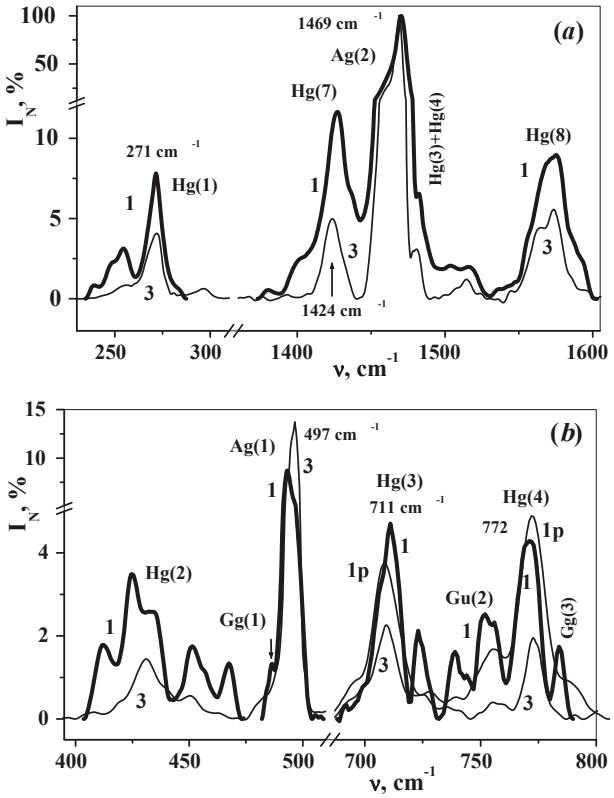

Fig. 2. Comparison of the vibrational bands normalized on line Ag(2) in the Raman spectra of nanofilms of fullerene C_{60} fabricated by the hot method of deposition (1), microfilms of fullerene C_{60} 2 microns in thickness (3), and nanofilms polymerized by diamine (1p) in the region of the bands Hg(1), Ag(2) and Hg(7,8) and bands Hg(2,3,4) and Ag(1) (*b*)

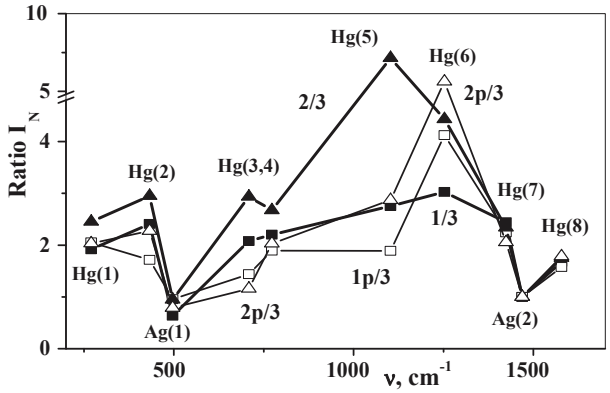

Fig. 3. Enhancement of active vibrations Hg(1–8) in the Raman spectra of the nanofilms of fullerene C_{60} in comparison with microfilms about 2 microns in thickness in the cases of the hot (1/3) and cold (2/3) deposition methods, as well as nanofilms polymerized by diamine (1/3 and 2p/3)

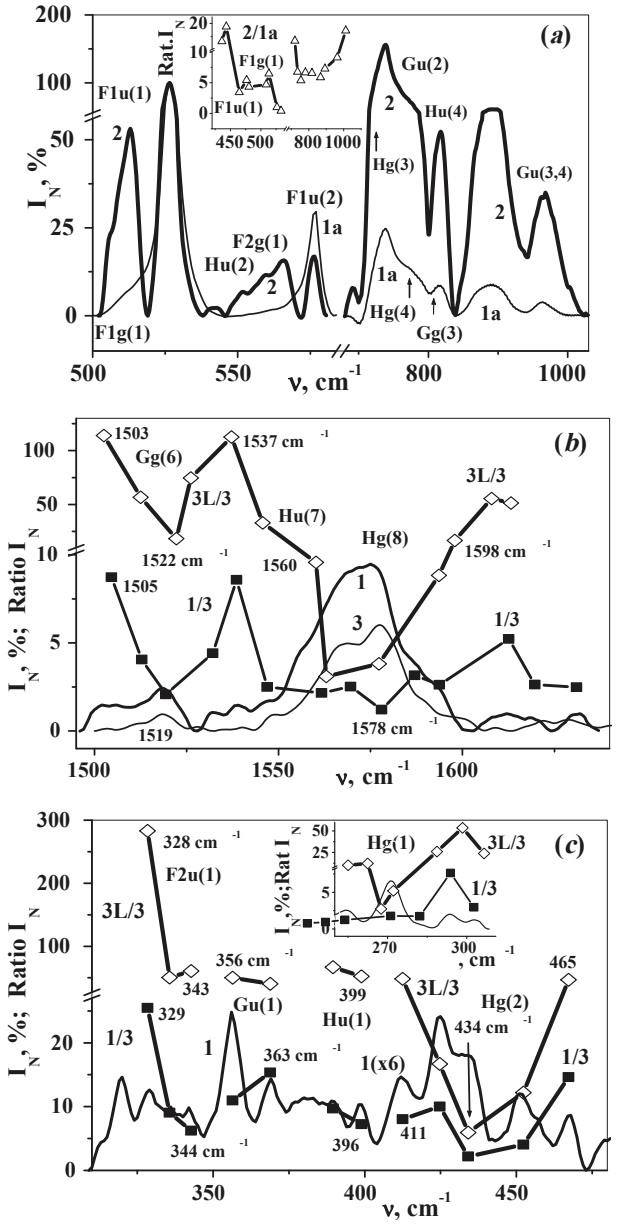

Fig. 4. The fragments of enhanced normalized IR absorption spectra (*a*) and Raman spectra (*b, c*) of the nanofilms of fullerene and the enhancement of the intensity of some "silent" and active vibrations in the vibrational spectra of nanofilms (curves with dark symbols), and microfilms after intense light irradiation (curves with open symbols) in comparison with the initial microfilms (*a, b, c*)

intense line $F_1u(1)$ with a frequency of 527 cm^{-1}. The gain enhancement of some inactive vibrations such as in IR spectrum of the nanofilm of fullerene C_{60} (spectrum 1) with the comparison of a microfilm 1.2 microns in thickness (spectrum 3a) is shown in Fig. 4. It is evident that some previously "silent" vibrations (e.g., Gu(2), Gg(3), Hu(4), $F_1g(1)$) became equal to and even exceed the absorption for the strongest IR line $F_1u(1)$. In the IR spectrum of C_{60} nanofilms, the weaker bands of inactive Hu(2) and $F_2g(1)$ vibrations also appeared, but the active infrared band $F_1u(2)$ is even suppressed. The majority of bands in the IR spectra of nanofilms increase by 5–20 times, as shown in the inset in Fig. 4, *a*. The examples of manifestations of inactive vibrations in the high-frequency and low-frequency RS ranges are shown in Fig. 4, *b*, *c*, respectively. Some of the identified spectral components of these vibrations with their degeneracy are shown in the same figures, where their frequencies are also indicated. Figure 4, *b* demonstrates the spectral dependences of the enhancement of inactive vibrations of C_{60} in the spectra of nanofilms, as well as the enhancement of the side spectral components of active vibrations such as Hg(1,2) Hg(8) in the comparison with a microfilm with $d = 2$ μm (curves with dark symbols). For comparison, in Fig. 4, *b*, we also show the increase of the vibrational bands in a microfilm 2 μm in thickness in the case of the strong focusing of the exciting radiation onto a spot 2 mm in diameter (curves 3L/3 with open symbols). In a vicinity of Hg(8), the highest-frequency inactive vibrations Gg(6) and Hu(7) appear, which is in a good agreement with data from [9, 10]. First of all, it should be noted that the side spectral components increase more than central components. This holds for both active and inactive vibrational bands. For example, for the active band Hg(8) in nanofilm 1 for strong focusing of the excitation radiation, the central part is enhanced by 3 times, and the side one by 10–17 times. This regularity is also manifested for the inactive band Gg(6). In nanofilm 1, the central component of this band at 1519 cm^{-1} increases by a factor of 2.1, and the side components increase by 8.8 times. Under the strong laser influence on the microfilm of fullerene C_{60}, the center of the band Gg(6) enhances by 18.2 times, and the side components by 112 times. In the low-frequency region between the Hg(1) and Hg(2), the bands of inactive vibrations $F_2u(1)$, Gu(1), and Hu(1) have been detected (see Fig. 4, *c*). The positions of these silent vibrations are in a good agreement with the results of quantum-chemical calculations (QCC) with regard for various degenera-

tions of these vibrations. We point out that, in some works [9, 10], the classification of these vibrations is not in agreement with QCC. Both for the vibration Hg(8) and low-frequency bands Hg(1) Hg(2), the regularity of the bigger enhancement of side components takes place. For example, for band Hg(2) in the spectrum of nanofilm 1, the central component enhances by 2.2 times, whereas the side ones by 10–15 times. In the case of strong laser irradiation, the center of band Hg(2) increases by 6 times, and the side components by 45–48 times.

Inset in Fig. 4, *c* shows a part of the Raman spectrum in a vicinity of the lowest-frequency band Hg(1) and the enhancement of some spectral components in nanofilms, including the case of the strong focusing of laser radiation. In the latter case, the center of Hg(1) band increases by 2.8 times, and the side components by 12–26 times. As for the high-band satellites of Hg(1) in the region 294–303 cm^{-1} [1, 2], they increase by 53 times. For the inactive vibrations, the observed spectral components in nanofilms enhance by 5–25 times, and, under a strong laser irradiation, the enhancement reaches 50–300 times even for microfilms.

3.3. Local induced electronic bands

According to Fig. 1, *a*, *b*, the less broad "islets" EBs appear in a vicinity of numerous vibrations apart from the very broad EB with half-widths more than $\delta\nu = 10^3$ cm^{-1}. Moreover, these additional EBs may be more intense than the main bands. For example, in a vicinity of the vibrational bands Hg(3,4) with Raman shifts 709 and 773 cm^{-1}, local EBs are stronger than those in a vicinity of the strongest Hg(1) band near 270 cm^{-1} (see Fig. 1, *a*, *b*). The subtraction of the local EB in the region of Hg(3,4), Ag(2), and Hg(7,8) vibrations for a microfilm of C_{60} polymerized by diamine is illustrated by Fig. 5, *a*, *b*.

One can see that the half-widths $\delta\nu$ of local EBs are about 100–200 cm^{-1}, which is substantially less than the half width of EB shown in Fig. 1, *a*, *b*, but considerably bigger than the half-widths of vibrational bands. The localization of the "islet" EB in a vicinity of the vibrations can be seen by the coincidence of a local VB 1424 cm^{-1} with a vibration Hg(7) in Fig. 5, *b*, confirming their relationship with vibrations and the VEI. Probably, an important role is played by the coincidence of the band Hg(7) with the IR active

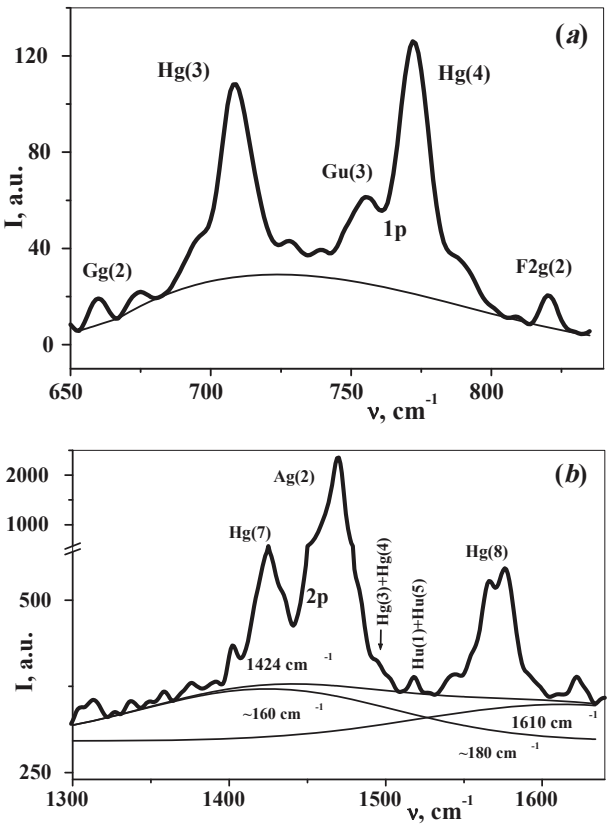

Fig. 5. Subtraction of vibrational induced local electronic bands (EB) in the Raman spectra of nanofilms of fullerite C_{60} in the case of the hot (*a*) and cold (*b*) methods of deposition and polymerization by diamine in the field of vibrational bands Hg(3,4) (*a*) Ag(2), Hg(7,8) (*b*)

vibration $F_1u(4)$ at 1429 cm^{-1}. The peak intensities of the considered local VB approach the maxima of narrow vibrational bands of C_{60}, and the integrated intensities of EB are considerably greater.

3.4. Discussion

It is very significant that the "islets" electronic bands are localized exactly in a vicinity of Hg(3) and Hg(7) associated with the main vibrational resonances Hg(1)+Hg(2) = Hg(3), 2Hg(3) = Hg(7). Due to these resonances, the thermal excitations of low-frequency modes Hg(1) and Hg(2) as a result of nonlinear interactions are converted initially into the medium-frequency vibration Hg(3) and then to the high-frequency vibration Hg(7). Due to the nonlinear processes under study and their associated vibrational-electronic interactions, the changes

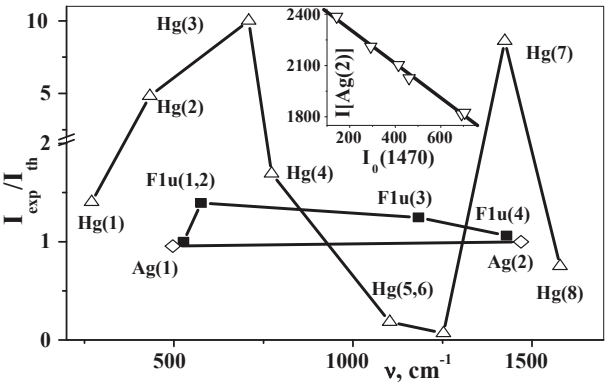

Fig. 6. The comparison of observed and calculated intensities of the Raman active Hg(j) bands (open symbols) and IR F_1u(1–4) bands (dark symbols) (b). The inset shows the peak intensely decrease for Ag(2) band as a function of $I_0(1470)$ in a vicinity of the current vibration

of electronic states take place. They manifest themselves in changes of the derivatives of the electronic polarizabilities with respect to the vibrational coordinates $d\alpha/dq$, which determine the intensity enhancement of the vibrational bands in the Raman spectra, and in the appearance of new electronic states in the vibrational field. The localization of broad electronic bands in the region of the most intense RS bands Ag(2) and Hg(7,8) (Fig. 1, b), as well as the displacements induced by EB under the influence of intense laser radiation in the region of overtones 2Ag(2), 2Hg(7, 8) also indicate a connection between the vibrational and electronic subsystems. The last point characterizes the increased interaction of the atomic and electronic subsystems (violation of the adiabatic approximation). The role of a strong VEI is confirmed also by the linear weakening of the intensities of Ag(2) bands in nanofilms together with the increase in the broad band intensity I_0 near band Ag(2), which is shown in the inset in Fig. 6. The obtained results are very important for the understanding of the essential differences between detected Raman intensities for a microfilm of fullerite C_{60} 2 microns in thickness and the results of QCC. These differences are summarized in Fig. 6. All experimental and theoretical intensities of bands Hg(i) and Ag(1,2) have been normalized on the corresponding values for band Ag(2), and the values for IR bands $F_1u(k)$, where $k = 1$–4, have been normalized on the most intense IR band $F_1u(1)$. For the totally symmetric vibrations of fullerene C_{60}, Ag(1,2), the QCC results are in good agreement with experiment. For IR active vibrations $F_1u(2,3)$, there is a small increase in the absorbance as compared with the results of calculations. Abnormal differences between experimental and calculated results have been established for bands of the Hg(j) type. In particular, the observed intensities of Hg(3) and Hg(7) bands are 8–10 times greater than the calculated ones, and the bands Hg(5,6) are weaker by more than 10 times (see Fig. 6). It is of importance that we detect experimentally the enhancement of exactly Hg(3) and Hg(7) bands associated with the vibrational resonances Hg(1)+Hg(2) = Hg(3), 2Hg(3) = Hg(7). This is a powerful argument in favor of developing a nonlinear vibration-electronic concept.

It is essential that the maximum ratio of the observed and calculated intensities of the vibrational bands $I_{\rm exp}/I_{\rm th}$ for the vibrations Hg(3) and Hg(7) in Fig. 6 are consistent with an increase in the intensities of these bands in nanofilms C_{60} in Fig. 3. Since the increases of the intensities of the vibrational bands in nanofilms are associated with NIVM and VEI, the detected differences of QCC with the experiment can be caused just by these phenomena. This shows a possible way of improving the QCC. This important conclusion is confirmed by a detailed analysis of changes in the intensities of Hg(3,4) bands. In accordance with the Raman spectra in Fig. 1, a, b, the bands Hg(3) and Hg(4) have close intensities, but QCC gives the intensity of Hg(4) vibration about 6 times higher than Hg(3) one. According to Fig. 2, b, the intensity of the band Hg(3) in nanofilm 1 higher than that for Hg(4), i.e., in good agreement with Fig. 3 (factor of 2/3). However, in Fig. 2, b, in nanofilms after the polymerization, when the total nonlinearity in nanofilms decreases, the band Hg(3) is weakened, and Hg(4) is enhanced (spectrum 1p). This is close to the results of QCC. This fact proves that the discussed differences are related to the nonlinear interaction of vibrational modes and strong VEI, which was not taken into account in QCC.

4. Conclusions

The observed abnormal enhancement of the vibrational bands in nanofilms of fullerene C_{60} is associated with a significant change in the electrophysical parameters of nanostructured objects as a result of weakening the symmetry and enhancing the anhar-

monicity and NEVM. This leads to increasing the VEI, which plays a significant role in nanostructures, but practically has not been studied till now. The significant role of vibrational-electronic interactions (VEI) is indicated by a number of factors:

1. Maximum of the broadband background in the Raman spectra of microfilms of fullerene C_{60} is achieved in the region of strong high frequency vibrations Ag(2) and Hg(7,8), closest to the electronic states. In the same area, the maximum of the broadband background of nanofilms of C_{60} is shifted after their polymerization by diamine N_2H_4.

2. The detection of the local background bands in the region of Hg(3) and Hg(7) vibrations associated with the vibrational resonances Hg(1) + Hg(2) = = Hg(3), 2Hg(3) = Hg(7), is the strong evidence of the discussed nonlinear vibration-electronic concept and the electronic origin of broad bands in the Raman spectra.

3. Abnormal enhancement of the intensities of active and inactive vibrations in Raman and IR spectra also associated with essential changes of electronic states due to a strong vibrational-electronic interaction.

4. Characteristically, not only the maximum difference between the calculated and observed intensities of the Hg($1 \div 8$) bands is achieved for the vibrations Hg(3) and Hg(7), but the band splitting for Hg($1 \div 8$) resulted from the isotopic lifting of a degeneracy is also achieved for the vibrations Hg(3) and Hg(7) [11] associated with nonlinear resonances.

On the whole, the obtained results clearly demonstrate the essential role of nonlinear wave interactions of the vibrational modes and VEI just for nanofilms of fullerenes C_{60}. However, it can be assumed that these regularities are characteristic of other nanostructured materials, as evidenced by our close results [12–14]. In conclusion, the discussed nonlinear vibrational-electronic concept can contribute, in our opinion, to the development of a new method of spectroscopy, which will provide information about the nonlinear vibration-electron dynamics and nonlinear changes in the quantum properties of the material media in addition to the vibrational dynamics.

1. M.E. Kornienko, M.P. Kulish, S.A. Alekseev, O.P. Dmitrenko, and J.L. Pavlenko, Ukr. J. Phys. **55**, 732 (2010).
2. N.E. Kornienko, N.P. Kulish, S.A. Alekseev, O.P. Dmitrenko, and E.L. Pavlenko, Optika Spektr. **109**, 742 (2010).
3. N.E. Kornienko, Visn. T. Shevchenko Nat. Univ. Kyiv. Ser. Fiz. Mat. 489 (2006); 248 (2008).
4. A.P. Naumenko, N.E. Kornienko, V.M. Yashchuk, V.N. Bliznyuk, and S. Singamaneni, Ukr. J. Phys. **57**, 197 (2012).
5. N.E. Kornienko, Quant. Electronics **12**, 1595 (1985).
6. N.E. Kornienko, Optika Spektr. **60**, 186 (1986).
7. N.E. Kornienko, M.F. Kornienko, A.P. Naumenko, and A.M. Fedorchenko, Optika Spektr. **60**, 650 (1986).
8. N.E. Kornienko and S.I. Mikhnitskiy, Ukr. Fiz. Zh. **42**, 726 (2002).
9. Zheng-Hong Dong, Ping Zhou, J.M. Holden, P.C. Eklund, M.S. Dresselhaus, and G. Dresselhaus, Phys. Rev. **48**, 2862 (1993).
10. K.-A. Wang, A.M. Rao, P.C Eklund, M.S. Dresselhaus, and G. Dresselhaus, Phys. Rev. **48**, 11375 (1993).
11. N.E. Kornienko,V.A. Brusnetsov, and T.L. Pavlenko, in *Fullerenes and Nanostructures in Condensed Matter* (A.V. Luikov Heat and Mass Transfer Institute, Minsk, 2013), p. 264.
12. N.E. Kornienko, L.L. Sartinskaya, A.V. Kutsay, and Ts. Yastrbskiy, in *Fullerenes and Nanostructures in Condensed Matter* (A.V. Luikov Heat and Mass Transfer Institute, Minsk, 2013), p. 257.
13. N.E. Kornienko, T.O. Busko, and N.P. Kulish, in *Fullerenes and Nanostructures in Condensed Matter* (A.V. Luikov Heat and Mass Transfer Institute, Minsk, 2013), p. 249.
14. M.E. Kornienko, N.L. Sheiko, O.M. Kornienko, and T.Yu. Nikolaenko, Ukr. J. Phys. **58**, 151 (2013).

Received 24.09.13

М. Корніенко, А. Науменко

ПІДСИЛЕННЯ КОЛИВАЛЬНИХ СМУГ ДЛЯ АКТИВНИХ ТА "МОВЧАЗНИХ" КОЛИВАНЬ В СПЕКТРАХ КОМБІНАЦІЙНОГО РОЗСІЯННЯ ТА ІЧ ПОГЛИНАННЯ НАНОПЛІВОК ФУЛЕРЕНІВ C_{60}

Р е з ю м е

Проведено порівняння інтенсивностей коливальних смуг (КС) в спектрах комбінаційного розсіяння (КР) та ІЧ поглинання наноплівок фулеренів C_{60} товщиною 150–250 нм та мікроплівок товщиною 1–2 мкм. У спектрах КР наноплівок виявлено підсилення максимумів активних КС Hg(1–8) у 2–7 разів порівнянно з мікроплівкою при невеликому ослабленні смуг Ag(1,2). Показано, що в КР та ІЧ спектрах наноплівок смуги неактивних для ікосаедричної симетрії I_h коливань типу Gg,u, Hu, $F_{1,2}g$, F_2u, а також бічні спектральні компоненти смуг Hg(1–8) зростають у 5–50 разів і більше. Спостережувані явища пов'язані зі значною зміною електрофізичних параметрів наноструктурних середовищ у результаті ослаблення симетрії і посиленням ангармонізму та нелінійної взаємодії коливальних мод. При полімеризації наноплівок діаміном (N_2H_4) зареєстроване по-

силення КС послаблюється, що пов'язано зі зменшенням коливальної нелінійності. Обговорюються відмінності спостережуваних в спектрах інтенсивностей КС з результатами квантово-хімічних розрахунків.

Н. Корниенко, А. Науменко

УСИЛЕНИЕ КОЛЕБАТЕЛЬНЫХ ПОЛОС ДЛЯ АКТИВНЫХ И "МОЛЧАЛИВЫХ" КОЛЕБАНИЙ В СПЕКТРАХ КОМБИНАЦИОННОГО РАССЕЯНИЯ И ИК ПОГЛОЩЕНИЯ НАНОПЛЕНОК ФУЛЛЕРЕНОВ C_{60}

Р е з ю м е

Сравниваются интенсивности колебательных полос (КП) спектров комбинационного рассеяния (КР) и ИК поглощения нанопленок фуллеренов C_{60} толщиной 150–250 нм и микропленок толщиной 1–2 мкм. В спектрах КР нанопленок обнаружено усиление максимумов активных КП Hg(1–8) в 2–7 раз по сравнению с микропленкой при небольшом ослаблении полос Ag(1,2). Показано, что в КР и ИК спектрах полосы неактивных для икосаэдрической симметрии I_h колебаний типа Gg,u, Hu, $F_{1,2}g$, и F_2u, а также боковые спектральные компоненты полос Hg(1–8) усиливаются в 5–50 раз и более. Наблюдаемые явления связаны со значительным изменением электрофизических параметров наноструктурных сред в результате ослабления симметрии и усиления ангармонизма и нелинейного взаимодействия колебательных мод. При полимеризации нанопленок диамином (N_2H_4) зарегистрированное усиление КП уменьшается, что связано с уменьшением колебательной нелинейности. Обсуждаются различия наблюдаемых в спектрах интенсивностей КП с результатами квантово-химических расчетов.